Palladium catalyzed C–H activation: Mass spectrometric approach to reaction kinetics in solution

Jiří Váňa,[†,‡] Thibault Terencio,[†] Vladimir Petrović,[†,‖] Orsolya Tischler,[§] Zoltán Novák,[§] and Jana Roithová*[,†]

† Department of Organic Chemistry, Faculty of Science, Charles University in Prague, Hlavova 2030/8, 12843 Prague 2, Czech Republic

‡ Institute of Organic Chemistry and Technology, Faculty of Chemical Technology, University of Pardubice, Studentská 573, 53210 Pardubice, Czech Republic

§ MTA-ELTE "Lendület" Catalysis and Organic Synthesis Research Group, Institute of Chemistry, Eötvös University, Pázmány Péter stny. 1/a, H-1117 Budapest, Hungary

‖ University of Kragujevac, Faculty of Science, Department of Chemistry, Radoja Domanovića 12, 34000 Kragujevac, Serbia

jana.roithova@natur.cuni.cz

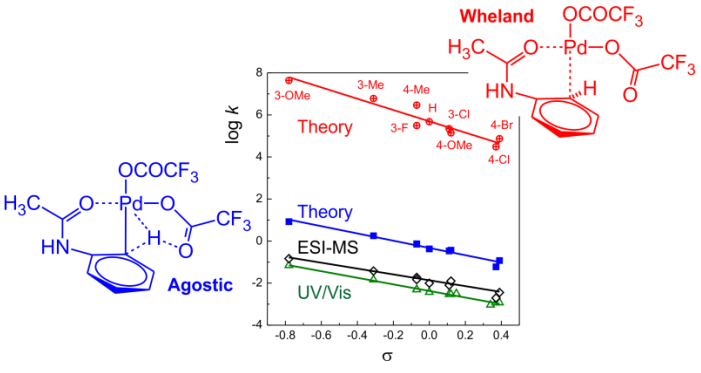

ABSTRACT

We report a new method for determination of rate constants of processes in solution using electrospray ionization mass spectrometry (ESI-MS). The investigated reaction is C–H activation of acetanilides by palladium(II)trifluoroacetate leading to stable organopalladium complexes. The rate constants can be determined from an experiment with a couple of differently substituted acetanilides being in competition activated by the palladium salt. The formed organopalladium complexes can be detected by ESI-MS. The time dependence is achieved by adding one of the acetanilides to the reaction mixture with a time delay. The kinetics can be then evaluated from the evolution of the ratio of the ESI-MS signals of differently substituted complexes as a function of the time delay. The Hammett analysis of the rate constants obtained for a series of *meta*- and *para*-substituted acetanilides provides the ρ value of -1.5, which is in agreement with values reported for similar C–H activations. We have investigated the very same reaction also with UV-Vis spectroscopy that gave us about three times smaller rate constants, but the same trend with the ρ value of -1.6. The rate constants determined by ESI-MS are directly linked to the occurrence of organopalladium complexes, whereas the UV-Vis data are associated with an absorption spectra change that could involve more reaction steps. DFT calculations support the interpretation of the reaction mechanism as cyclopalladation and provide the ρ value in the same range. The rate determining step corresponds to the agostic C–H transition structure.

KEYWORDS

Agostic mechanism, C–H activation, cyclopalladation, Delayed reactant labeling, DFT calculations, Electrospray ionization artifacts, Hammett analysis, Wheland intermediate

INTRODUCTION

C–H activation reactions represent one of the challenges in current organic synthesis.[1] Most of the catalysts are based on transition metals.[2] The catalysts have to be reactive enough to activate strong C–H bonds and at the same time provide a high degree of selectivity to form one dominant product. One of the approaches to tackle the dilemma of high reactivity vs. high selectivity relies on employment of directing groups.[3,4] The directing group brings the transition metal and its ligands to the vicinity of the given C–H bond. Understanding of the role of the metal as well as the ligands is essential for rational catalysts design. Does the C–H activation proceed by cyclometalation or is it rather oxidative addition? These and other questions are in focus of numerous mechanistic studies that accompany the recent research boom in the development of C–H activation reactions.[5]

Several reaction mechanisms were proposed for the directing group assisted C–H activation. The pioneering work was done by Ryabov et al.[6] who suggested electrophilic substitution via Wheland-type intermediate followed by intramolecular deprotonation by acetate coordinated to the palladium via the six-membered transition state (Figure 1, **A**). Davies and Macgregor suggested that the hydrogen migration is assisted by the metal (Figure 1, **B**).[7] Finally, an alternative scenario involving four-membered transition state was proposed by Gomez et al. (Figure 1, **C**).[8] In addition, classical mechanisms such as oxidative addition,[9] electrophilic substitution (S_E3),[10] or σ-bond metathesis (SBM)[11] were considered, too. The determination of rate constants for this process in dependence of the substrate substitution can certainly help in disentangling the possible scenarios and in determining the actual reaction mechanism.

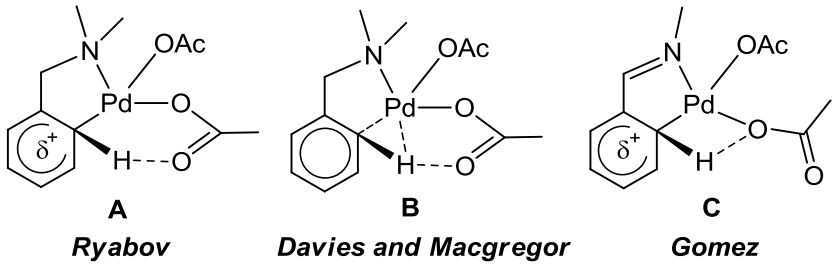

Figure 1. Proposed transition states for cyclopalladation.

The methods of choice for kinetic studies would be UV-Vis spectroscopy,[12] NMR,[13] IR,[14] or calorimetry.[15] However, for metal catalyzed reactions, these methods could fail. UV-Vis spectroscopy requires diluted solutions that can distort the reaction conditions. NMR spectroscopy can be complicated for paramagnetic metals. In addition, the concentration of metal catalyst is usually very low in comparison to the reactants, which makes the signal evaluations unreliable. We present here a new method for determination of rate constants using electrospray ionization mass spectrometry (ESI-MS).

The main advantage of ESI-MS is high sensitivity and large dynamic range that permits selective detection of even a very low abundant species.[16] The main disadvantage is the non-linear ion transfer response of ESI to the concentration of the given species in solution.[17] The concentration can be thus determined only using isotopically labelled standards.[18] For investigation of reaction intermediates, we have recently introduced a new method denoted as Delayed reactant labeling.[19,20] We use isotopic labeling in situ with a trick of different reaction times for labeled and unlabeled reactants.

The mutual evolution of equivalent, labeled and unlabeled signals in the ESI-MS spectrum reflects the kinetics of the relevant species in solution. In the present work we will test this method for determination of the rate constants associated with the formation of palladium intermediates.

The method is demonstrated for the C–H activation reaction of substituted acetanilides with palladium(II)acetate in dichloromethane (DCM) accelerated by the addition of trifluoroacetic acid (TFA) (Scheme 1). This reaction is the first reaction step in palladium catalyzed functionalizations on acetanilide skeleton.[21] Instead of isotopic labeling, which is problematic in this case due to the rich isotopic pattern of palladium containing species, we decided to use different substitution introduced to the phenyl ring of the acetanilide substrate (i.e. *m/z* differences are sufficient so that the isotopic profiles do not overlap).

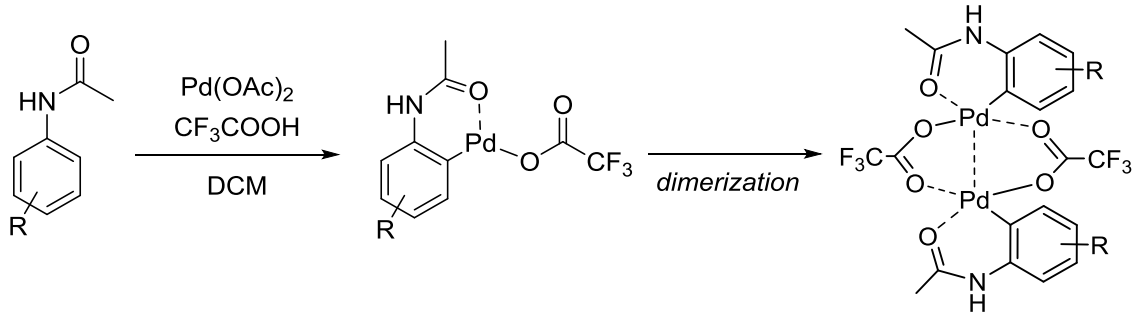

Scheme 1. C–H activation of acetanilides catalyzed with palladium(II)acetate and TFA.

EXPERIMENTAL AND COMPUTATIONAL DETAILS

Preparation of reaction mixtures. The absolute rate constants were determined for 4-bromoacetanilide (**R_1**). The reaction was initiated by addition of a solution containing 0.1 mmol of **R_1** dissolved in 0.2 ml of dichloromethane (DCM) with 12 μL of trifluoroacetic acid (TFA), to the mixture of 5 mol% (0.005 mmol) of $Pd(OAc)_2$[22] (**C**) in 10 μL of DCM containing 10 μL TFA, which was reacted for twenty seconds. After a given time delay (t_d), the analogous reaction mixture containing acetanilide (**R_2**) was assembled in the same way as in the case of substrate (**R_1**), and immediately added to the first reaction mixture. The reaction is completed after 20 minutes (no further changes in the relative concentration of palladium complexes can be detected, see Figure S1). In order to account for possible experimental deviation, we set the total reaction time to 30 min. After 30 min, the reaction mixture was diluted 100 times by dichloromethane and analyzed by ESI-MS.

UV-Vis experiments. The kinetic experiments were run on Hewlett Packard 8453 diode array spectrophotometer in 0.5 ml cuvette with optical path 1 cm at the temperature 25 °C. The palladium was preactivated by dissolving of 2.75 mg of $Pd(OAc)_2$ (0.0125 mmol) in 135 μL of DCM and addition of 35 μL of TFA. After one minute this solution was injected to a cuvette containing 0.25 mmol of acetanilide dissolved in 370 μL of DCM and the kinetic was followed. The rate constants were obtained by fitting the absorbance changes at 520 nm by the first order kinetic model.

Mass spectrometry experiments. The experiments were performed with Finnigan LCQ Deca ion trap mass spectrometer equipped with an ESI source operating in the negative- or the positive mode.[23] The reaction mixtures were diluted by dichloromethane to approximate concentration $5 \cdot 10^{-5}$ mol/L and were introduced to the ESI source through a fused-silica capillary by a syringe pump at a rate of 30 $\mu L \cdot min^{-1}$. The operating conditions were set as follows: spray voltage 5.0 kV, capillary voltage 0 V, tube lens offset 100 V, heated capillary temperature 220 °C. All of the mass spectra were recorded from m/z 50 to m/z 2000.

Electrospray ionization and ion transfer responses. In the beginning, we have expected that the ESI responses for palladium complexes bearing differently substituted acetanilides will be very similar (i.e. similar concentration of complexes in solution will lead to similarly abundant ESI-MS signals). During the experiments it had revealed that the ESI efficiencies were actually drastically different for different complexes, therefore we had to account for it in the modelling (see below). In order to demonstrate the large effect of the substitution at the aromatic ring on the ionization and ion transfer to the gas phase, we have performed a series of experiments shown in the Supporting Information (Figures S2 – S9).

DFT calculations. All calculations were performed using the B3LYP density functional theory method as implemented in Gaussian09[24] with the D3 dispersion term using the Becke-Johnson damping function.[25] The basis set was a combination of the SDD pseudopotential model for palladium[26] and 6-311++G** for all other atoms. The rate constants for the C–H activation were calculated according to the Eyring equation.

Kinetic model (method description). The relative rate constants for the irreversible parallel reactions (1) and (2), in which reactants R_1 and R_2 (with identical concentrations) compete in reaction with C, can be simply determined from the relative concentrations of the products P_1 and P_2, when the reaction is

completed (Equation 1).[27]

$$R_1 + C \xrightarrow{k_1} P_1 \qquad (1)$$
$$R_2 + C \xrightarrow{k_2} P_2 \qquad (2)$$

$$\left(\frac{[P_1]}{[P_2]}\right)_{fin} = \frac{k_1}{k_2} \qquad (1)$$

For the determination of the absolute rate constants, we have to introduce a time variation to the experiment. We have achieved this by adding the second reactant R_2 with a certain time delay t_d to the reaction mixture (*i.e.* we vary the reaction time of R_2 with respect to R_1).[19,28] First, the reaction is set only with reactant R_1 and a half of the total amount of C and let to react for time t_d. After t_d elapses, the concentrations of $[C]_{td}$ and $[P_1]_{td}$ are (we assume the pseudo first-order reaction kinetics):

$$[C]_{t_d} = 0.5[C]_0\, e^{-k_1 t_d} \qquad (2)$$
$$[P_1]_{t_d} = 0.5[C]_0(1 - e^{-k_1 t_d}) \qquad (3)$$

At time t_d, the second half of the reactant C and reactant R_2 are added; the reaction is left to run until all reactant C is consumed ($[P_1]_{fin} + [P_2]_{fin} = [C]_0$). The concentrations of $[P_1]_{fin}$ and $[P_2]_{fin}$ can be expressed as:

$$[P_1]_{fin} = [P_1]_{t_d} + 0.5[C]_0\,(1 + e^{-k_1 t_d})\frac{k_1}{k_2+k_1} \qquad (4)$$
$$[P_2]_{fin} = 0.5[C]_0\,(1 + e^{-k_1 t_d})\frac{k_2}{k_2+k_1} \qquad (5)$$

product ratio is thus:

$$\left(\frac{[P_1]}{[P_2]}\right)_{fin} = \frac{k_1}{k_2} + \left(1 + \frac{k_1}{k_2}\right)\frac{1-e^{-k_1 t_d}}{1+e^{-k_1 t_d}} \qquad (6)$$

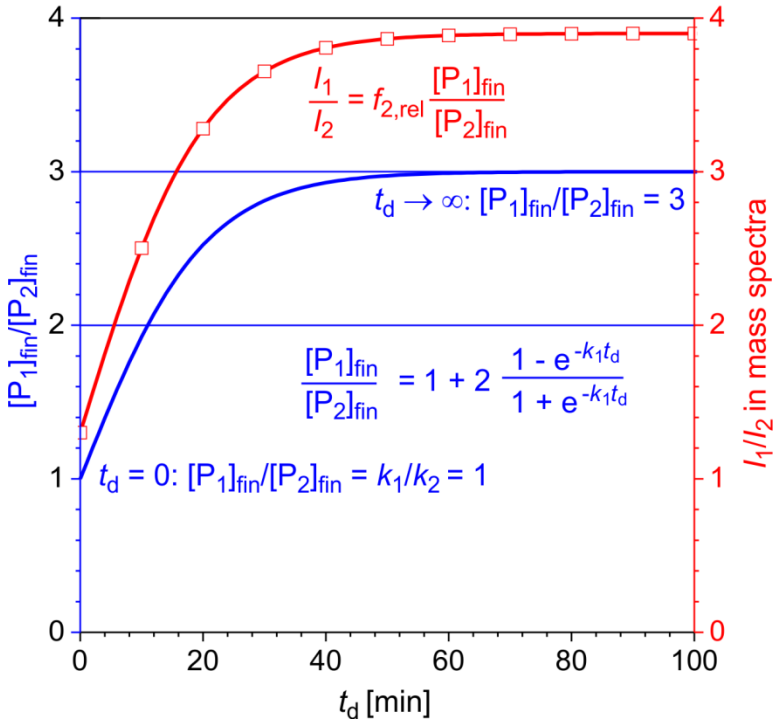

Figure 2. An ideal experiment with $k_1 = k_2 = 0.1$ min^{-1}. The blue curve shows the evolution of the concentration of the products in dependence of the time delay t_d. The product ratio varies between the extremes for $t_d = 0$ being 1 (*i.e.* reactant C is transformed in 1:1 ratio to P_1 and P_2) and for being $t_d = \infty$ being 3 (the first half of C is transformed to P_1 and the second half of C is transformed in 1:1 ratio to P_1 and P_2). In mass spectra, the ratio of the corresponding signals is multiplied by the relative response factor $f_{2,rel} = f_2/f_1$, so we would measure the points on the red curve (here: $f_{2,rel} = 1.3$). Fitting of the red points using Eq. 8 gives the values of the rate constants as well as the relative response factor $f_{2,rel}$.

If the relative signal intensities of the product complexes would be proportional to their relative concentrations (*i.e.* $[P_1]/[P_2] = I_{P1}/I_{P2}$, where I_{Pi} corresponds to the intensity of the signal of P_i in a mass spectrum), then Equation (6) could be used to fit the experimental results and thus to determine k_1 as well as k_2. In general, however, we cannot expect the same efficiency of ESI and ion transfer for different complexes and thus $[P_1]/[P_2] \neq I_{P1}/I_{P2}$ (for more details see Figures S2-S9). In order to correct for this nonlinearity, we introduce the ESI response factors: $I_{P1} = f_1[P_1]$ and $I_{P2} = f_2[P_2]$.

$$\frac{I_{P1}}{I_{P2}} = \frac{f_2[P_1]}{f_1[P_2]} = f_{2,rel}\frac{k_1}{k_2} + f_{2,rel}\left(1 + \frac{k_1}{k_2}\right)\frac{1-e^{-k_1 t_d}}{1+e^{-k_1 t_d}} \qquad (7),$$

where $f_{2,rel}$ gives relative ESI response of P_2 with respect to P_1. The obtained ratio of signal intensities of

P_1 and P_2 in the mass spectra is therefore fitted with the function

$$\frac{I_{P1}}{I_{P2}} = A + B\,\frac{1-e^{-k_1 t_d}}{1+e^{-k_1 t_d}} \qquad (8).$$

The fits provide directly k_1. The values of k_2 and $f_{2,\mathrm{rel}}$ can be derived as:

$k_2 = \frac{k_1(B-A)}{A}$ and $f_{2,rel} = B - A.$

RESULTS AND DISCUSSION

Reaction kinetics by ESI-MS experiments. The absolute rate constants were determined using 4-bromoacetanilide as the reference reactant, because it reacts slowest and thus provides the longest time delay axis (for details see the Kinetic Model part). Figure 3 shows a typical negative mode ESI-MS spectrum obtained after the competition reaction was completed. The spectrum corresponds to the competition between 4-bromoacetanilide (**R_1**) and unsubstituted acetanilide (**R_2**) added with a delay of 1000 s. We can see three types of palladium complexes; all of them correspond to the products of the C–H activation reaction (Figure 3). The most abundant signals correspond to the binuclear $[(R\text{-}H)_2Pd_2(CF_3COO)_3]^-$ anions, followed by the mononuclear $[(R\text{-}H)Pd(CF_3COO)_2]^-$ and $[(R\text{-}2H)Pd(CF_3COO)]^-$ complexes, where R corresponds to either **R_1** or **R_2**. The structure of the $[(R\text{-}H)_2Pd_2(CF_3COO)_3]^-$ complex with R being the unsubstituted acetanilide was confirmed by infrared multiphoton dissociation (IRMPD) spectroscopy (Figure S12).[29] We have confirmed that (R–H) corresponds to the C–H activated complex and not to the *N*-deprotonated amide by comparison of the IRMPD spectrum with DFT predicted spectra for both isomers. The experimental spectrum of $[(\mathbf{R_2}\text{-}H)_2Pd_2(CF_3COO)_3]^-$ is in perfect agreement with the theoretical spectrum of a dimer with C–H activated aromatic ring (Figure S12A). Theoretical calculations also suggest that the dimers formed by the *N*-deprotonated anilides lie more than 150 kJ mol^{-1} higher in energy than the complexes with the C–Pd bond. For more details see the Supporting Information. In the following, we will assume that the dimeric complexes observed by ESI-MS correspond to the C–H activated acetanilides.

There is a fast equilibrium between dimeric palladium complexes. It was confirmed by an experiment in which two different synthetically prepared homodimeric complexes were mixed together and ESI-MS spectrum was measured immediately after the mixing (see Figure S9). The signals corresponding to homodimers and heterodimers were observed in the statistical ratio. The relative

abundance of palladium complexes in the dimeric form in the MS spectrum should therefore reflect (after correction on ESI response) their concentrations in solution. Monomeric complexes can be also present in solution, but they can be also formed by fragmentation of dimeric complexes (see Figures S10-S11). To minimize a possible fragmentation during the ESI process, we have measured at very soft ionization conditions. Signals of dimers and monomers were evaluated separately as well as together (Table 1 and Tables S2-S4 in the Supporting Information). All treatments lead to similar results; the values obtained from all data together have the smallest experimental error and these data are therefore used in further evaluation.

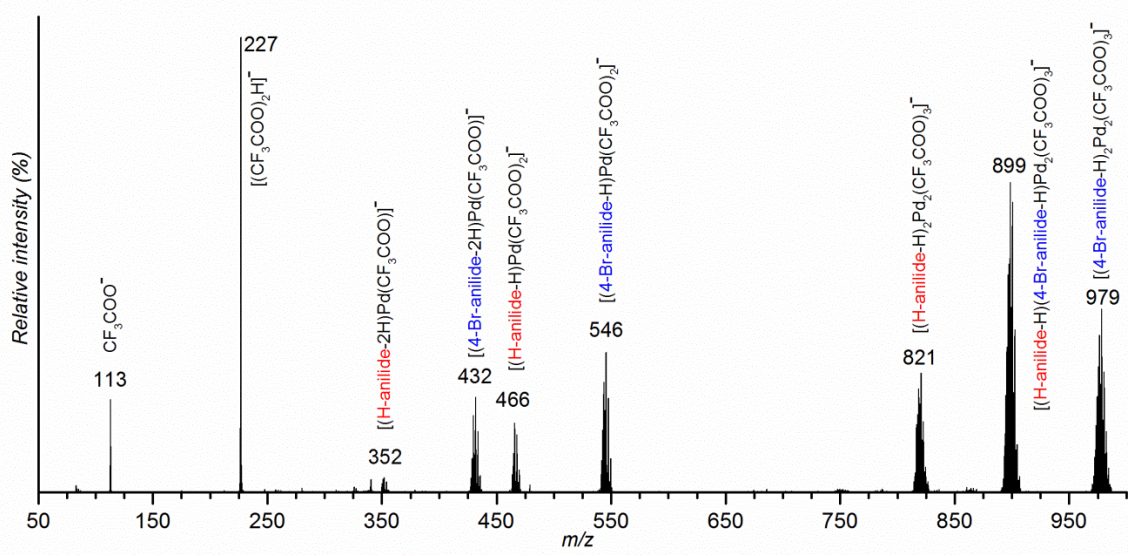

Figure 3. The ESI-MS spectrum in the negative mode for the complete reaction mixture containing acetanilide (red) and 4-bromoacetanilide (blue) with time delay 1000 s.

The evaluation of the relative abundance of the monomers according to Equation 8 has an advantage that we obtain the relative ESI response factor $f_{2,\mathrm{rel}}$ directly associated with the given species (Figure 4). The values can reflect not only the relative ionization responses, but can also cover a possible contribution of monomers formed by the fragmentation of the dimers. The same evaluation of the data for the dimers or for all relevant species together provides $f_{2,\mathrm{rel}}$ values that combine several factors together, and the values do not have straightforward interpretation. We therefore list only $f_{2,\mathrm{rel}}$ values obtained from the fitting of the data for monomers. Our kinetic model assumes that the reaction follows the (pseudo)first order kinetics (the anilides are in 20fold excess and trifluoroacetic acid in

60fold excess). This is true only when the trifluoroacetic acid and palladium(II)acetate are mixed together at least 20 s in advance before addition to acetanilide. If this palladium catalyst preactivation is not done, a preequilibrium reaction occurs and the obtained dependences cannot be easily interpreted.

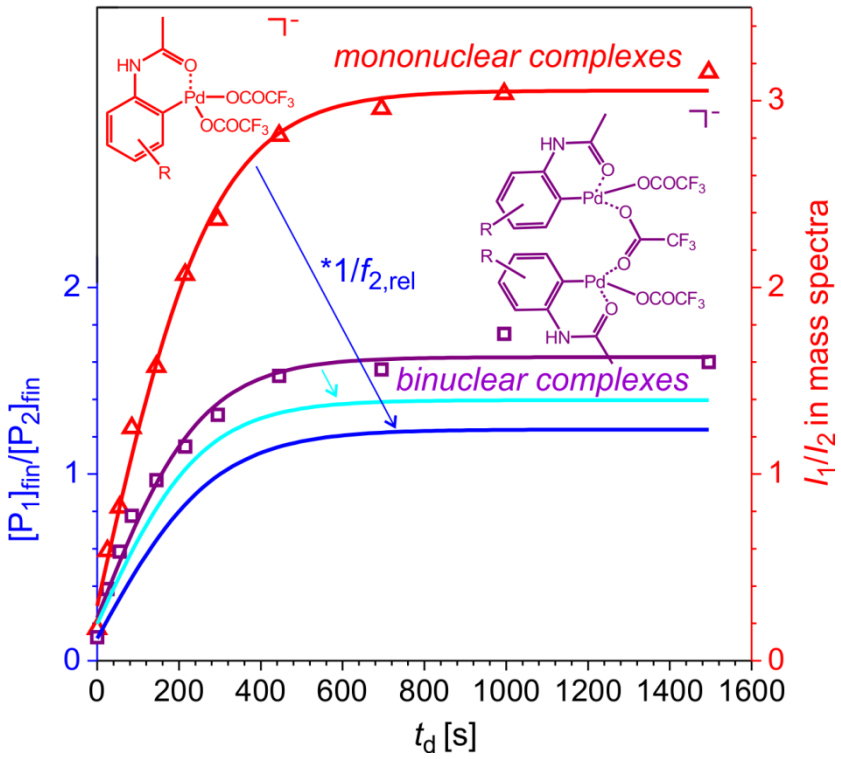

Figure 4. The experimental data and their fitting with Equation 8 for $\mathbf{R_1}$ being 4-bromacetanilide and $\mathbf{R_2}$ being 3-methylacetanilide. The symbols show the ratios of detected signals of $[(\mathbf{R_1}\text{-H})Pd(CF_3COO)_2]^-$ to $[(\mathbf{R_2}\text{-H})Pd(CF_3COO)_2]^-$ (red triangles) and $([(\mathbf{R_1}\text{-H})_2Pd_2(CF_3COO)_3]^- + 1/2\ [(\mathbf{R_1}\text{-H})(\mathbf{R_2}\text{-H})Pd_2(CF_3COO)_3]^-)$ to $([(\mathbf{R_2}\text{-H})_2Pd_2(CF_3COO)_3]^- + 1/2\ [(\mathbf{R_1}\text{-H})(\mathbf{R_2}\text{-H})Pd_2(CF_3COO)_3]^-)$ (violet squares). The corresponding lines are the fits of the experimental data using Eq. 8. The fitting gives relative ionization response factor that can be used to obtain the tentative ratio of the concentrations of the complexes in solution. The blue curve is for the monomers and the cyan curve for the dimers. We assume that all complexes are in equilibrium and thus both curves should be identical. The difference is given by the experimental and fitting error.

Table 1. Comparison of rate constants obtained by different methods.[a]

	ESI-MS			UV-Vis	Theoretical 1[c]	Theoretical 2[c]
substituent	k_1 (4-Br)	k_2	$f_{2,rel}$	k_{obs}	k_{theor}	k_{theor}
	10^{-3} s^{-1}			10^{-3} s^{-1}	10^{-1} s^{-1}	10^{5} s^{-1}
H	6.4±0.7	20±3	2.3±0.2	7.5±0.3	4.3	4.7
4-OMe	7.1±0.6	25±5	3.4±0.7	5.9±0.2	3.7	1.4
3-OMe	8.8±1.5	146±16	2.1±0.6	69.6±9.1	84	436
4-Me	7.1±1.1	38±6	1.6±0.4	9.9±0.7	7.5	29
3-Me	7.1±0.9	38±7	2.6±0.2	14.6±2.1	18	60
4-Cl	7.5±2.2	4.0±1	0.6±0.2	2.3±0.1	0.6	0.3
3-Cl	7.1±0.4	8.0±0.1	0.7±0.1	3.0±0.1	3.4	2.2
3-F	7.9±0.3	15±1	0.6±0.2	5.0±0.7	7.1	3.1
3-Br				3.9±0.1		
4-F				1.9±0.1		
4-Br		7.4±0.7[b]		2.4±0.1	1.2	0.7

[a] The experimental values are given with standard deviations.

[b] This value is an average of k_1 values determined in all experiments.

[c] The activation energy was obtained as the difference between the energy of **TS4b/5** and the minima **2a** (Theoretical 1 values) or between the energy of the Wheland intermediates **4b** and the minima **2a** (Theoretical 1 values); see below.

Table 1 lists the rate constants k_1 and k_2 determined as an average of the fittings of the sum of MS signals detected for mononuclear and binuclear complexes. The $f_{2,rel}$ factors correspond only to the mononuclear complexes (see Tables S2-S4). The rate constant for the C–H activation of 4-bromoacetanilide was determined as $k_1 = 7.4 \pm 0.7$ (10^{-3} s^{-1}). The determined rate constants can be used for the construction of a Hammett plot and to evaluate the given reaction mechanism (Figure 5). The substitution groups at the phenyl ring affect the C–H activation reaction by their electronic properties. They also affect the electronic properties of the directing acetyl group and thus the coordination of the substrate to the palladium catalyst. The second effect is considered as much less pronounced than the first one and for the sake of clarity, we neglected it in the construction of the Hammett plot. Based on these assumptions, the σ_m constants were used for 4-substituted acetanilides and σ_p^+ for 3-substituted ones. The 4-substituted acetanilides and unsubstituted acetanilide itself have two equivalent C–H bonds

in the *ortho* positions to the acetylamino substituent and therefore the observed rate constants were divided by two for the Hammett evaluation. The 3-substituted acetanilides undergo C–H activation only in the *para* position to the additional substituent and thus only one C–H bond can be activated.

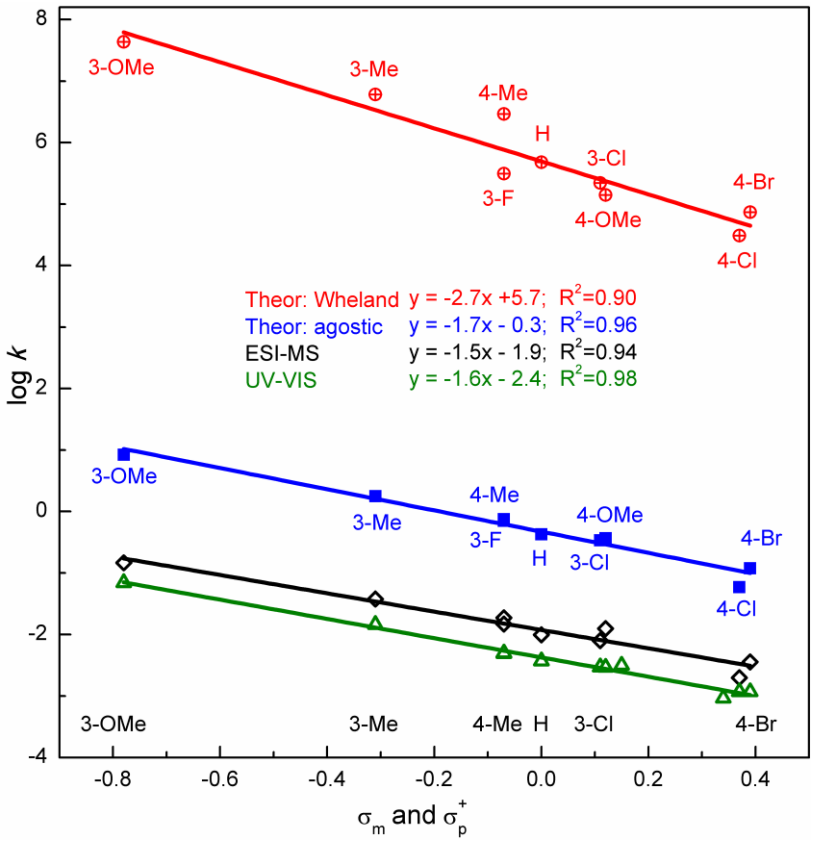

Figure 5 - Comparison of the Hammett plots constructed from the rate constants obtained from the fitting of the ESI-MS data (black), UV-Vis data (green) and theoretical calculations in the gas phase (blue: rate constants for the energy barrier calculated as energy difference between **TS4b/5** and **2a**; red: rate constants calculated for the gedanken experiment in which the pre-activated complex **4b** would represent the rate barrier; see below).

The Hammett plot shows a nice correlation of the experimental data (black points) with the ρ value of -1.5. The negative slopes are in accordance with the proposal that palladium acts as an electrophilic species, and thus the reaction is accelerated by electron donating substituents.

Reaction kinetics by UV-Vis experiments. As a benchmark experiments, we have measured kinetics of the same system by UV-Vis spectroscopy. The reaction was followed under very similar conditions as during the mass spectrometry experiments. The measured spectra (Figure S34) show a decrease of the absorbance in the range 460-620 nm. This change is directly observable as a color change from brown to yellow. The first spectrum of the kinetics nicely matches a spectrum of independently

prepared mixture of palladium acetate and trifluoroacetic acid (Figure S35). In the end of the experiment, the spectra closely resemble the spectrum of a solution prepared by dissolution of independently prepared binuclear palladium complexes bearing deprotonated acetanilides as ligands.[30] The absorbance changes at 520 nm were fitted by the first order kinetic model to obtain the observed rate constants k_{obs} (see Table 1 and Tables S5-S6 in Supporting Information).

The Hammett plot shows a very good correlation with the slope of -1.6, which nicely reproduces the value obtained from the MS experiments and thus the effects of the substituents. The determined rate constants are about three times smaller than those determined by the mass-spectrometry experiments. The explanation could stem from the fact that the UV-Vis experiments provide the observed rate constants and these could be composed from more individual rate constants (precomplexation, C–H activation, dimer formation).

Reaction kinetics by DFT calculations. To associate the determined rate constants with a reaction pathway, we investigated the C–H activation step also theoretically. We have shown previously that the palladation most probably proceeds according to the Macgregors agostic model[7] with the six-membered transition state and metal assisted hydrogen transfer.[5b] We will assume here only C–H activation within neutral monopalladium complexes with two trifluoroacetate ligands.

We have first investigated the structure of a complex between acetanilide and palladium trifluoroacetate. Palladium can coordinate either to the oxygen or to the nitrogen atom of the amide function (structures **1** and **2a** in Figure 6). The coordination to the nitrogen atom can be further associated with a hydrogen rearrangement leading to the imidic acid form of the complex (**3** in Figure 6). Palladium is in all structures bidentally coordinated by one of the trifluoroacetate ligands and monodentally by the other. The structures are further stabilized by hydrogen bonding between the monocoordinated trifluoroacetate and the acidic hydrogen of acetanilide. The most stable structure is the one with the imidic acid form of acetanilide. The energy barrier for the rearrangement of the *O*-coordinated palladium complex to the most stable form is calculated as 78 kJ mol^{-1} (see Figure S37). The energy barrier may be lower, if solvent molecules favorably assist the hydrogen shuttling reaction.

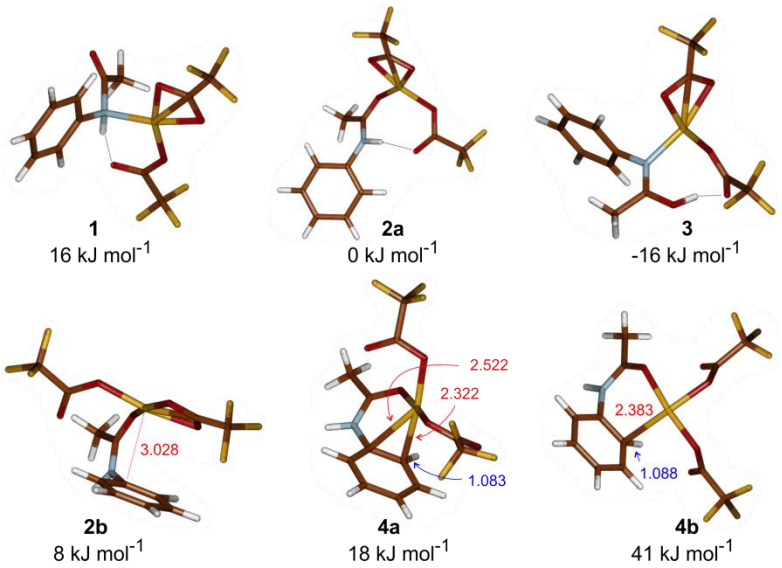

Figure 6. Isomers of a complex between acetanilide and palladium trifluoroacetate. The relative energies refer to Gibbs energies at 298 K in the gas phase. The numbers are distances in Å, red refers to the Pd–C distance and blue to the C–H distance.

The C–H activation step proceeds from the *O*-coordinated isomer **2**. This complex can adopt several conformers. Structure **2b** is only 8 kJ mol^{-1} higher in energy than the most stable conformer **2a**. Instead of hydrogen bonding it is stabilized by a dispersion interaction with the aromatic ring. The interaction between palladium and the aromatic ring leads to complexes **4a** and **4b**. In the π complex **4a**, palladium coordinates between *ipso* and *ortho* carbon atom with a short Pd–C distance (2.322 Å). The hydrogen atom in the *ortho* position has the same C–H bonding distance as the rest of the hydrogen atoms in the ring and the dihedral angle with respect to the ring is 168°. In the second complex **4b**, palladium coordinates only to the *ortho* carbon atom and the Pd–C distance is larger than in **4a** (2.383 Å). The C–H bond in the *ortho* position is slightly prolonged with respect to the other C–H bonds of the ring (1.088 Å vs. 1.083 Å). The dihedral angle of the C–H bond with respect to the ring is 170°. This complex lies considerably higher in energy than the remaining conformers (see Figure 6) and it is the isomer that is on the pathway to the C–H activation (Figure 7). With respect to its geometry, this complex cannot be denoted as a σ complex. In fact, in the σ-π continuum it lies closer to the geometry of a π complex.[31] With respect to its geometry, prolonged C–H bond and high relative energy, we denote the **4b** complex as a pre-activated complex of a Wheland-type intermediate.

The transition structure for the C–H activation reaction contains a much shorter Pd–C bond (2.109 Å) than in **4b** and the hydrogen atom is in between the carbon atom and the accepting oxygen atom of trifluoroacetate. The distance between the transferred hydrogen atom and palladium in 2.097 Å. The typical Pd–H bond is about 1.55 Å.[32] The sum of the van der Waals radii is 2.83 Å (Pd: 1.63 Å,

H: 1.2 Å). Hence, the palladium-hydrogen distance suggests a bonding between the atoms. The hydrogen transfer is thus mediated by the palladium atom.

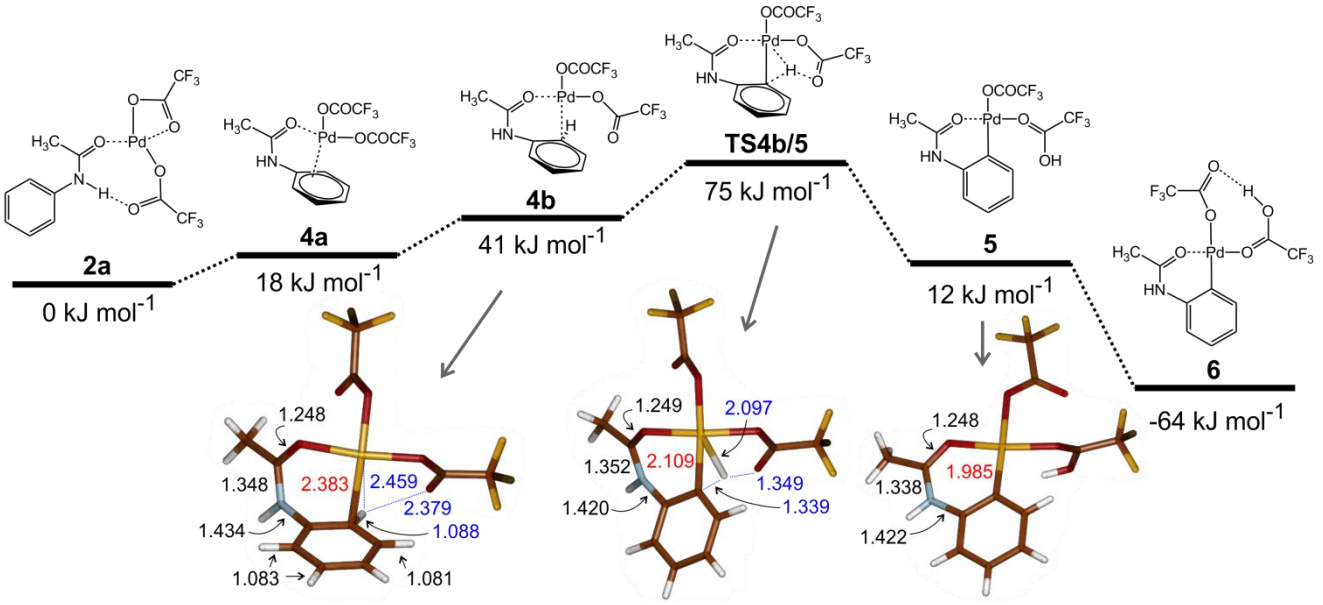

Figure 7. Energy profile (relative Gibbs energies at 298 K in kJ mol^{-1}) for C–H activation of acetanilide by palladium trifluoroacetate. The stick models are fully optimized while the chemical drawings are provided as a representative view (xyz coordinates of all points can be found in the SI). The values are bond distances in Angströms, the red numbers refer to the Pd–C distance, the blue numbers give the distances to the transferred hydrogen atom.

The transition structure is analogous to what was found by Davies et al. for the C–H activation of dimethylbenzylamine.[7] Nonetheless, their transition pathway leads to an agostic C–H intermediate with an even shorter Pd–H bonding distance (less than 2.0 Å). The Pd–H distance in our pre-activated complex **4b** is 2.459 Å which is still in the range of the overlap of the van der Waals radii, but the interaction is much weaker than in the transition structure and definitively much weaker than in the suggested agostic C–H intermediate. The reaction pathway for C–H activation of acetanilide therefore does not lead via agostic C–H intermediate, but rather via a Wheland type intermediate. The transition state that determines kinetics has, however, clearly agostic structure.

We have studied this reaction pathway for all substituted acetanilides and obtained analogous results (see the Supporting Information). For comparison with the experiment, we have also included solvation effect of dichloromethane by the PCM solvation model.[33] These calculations lead to qualitatively similar results, but the calculated rate constants are much larger (*cf.* Figure S39). It is given by a much larger free solvation energy obtained for transition states **TS4b/5** (as well as for **4a** and **4b**) compared to the minima **2a**, **2b**, or **3**. We assume that this effect is most probably and artifact of the PCM model (see Figure S38). Therefore, these results can be found in the SI, but we will discuss the results obtained in the gas phase here.

Similar to the experiments, we have determined the rate constants for the C–H activation from the calculations according to the Eyring equation and constructed the Hammett plot. If we assume the activation energy as the difference between the complex with *O*-coordinated acetanilide **2a** and the transition structure **TS4b/5**, then we obtain results shown in blue in Figure 5. The rate constants are larger than those obtained in the experiment, but it can be explained by the fact that we should have a mixture of palladium complexes with *O*- and *N*-coordinated acetanilide and only the former can lead to C–H activation. The pre-equilibrium reaction would thus lead to a decrease of the observed rate constant. The trend of the theoretical Hammett plot (ρ = - 1.7) is perfectly consistent with the experimental results.

Reaction mechanism. The values of the reaction constants ρ obtained from both experiments (-1.5 and -1.6) and theory are in a similar range as Ryabov`s value (ρ = -1.6) obtained for *ortho*-palladation of *N*,*N*-dimethylbenzylamines determined by spectrophotometric measurements in the UV-Vis range.[6] Yu and coworkers determined the constant ρ = -0.74 for palladium-catalyzed C–H acylation of *N*-aryl amides with aldehydes using *tert*-butyl hydroperoxide with the *ortho*-palladation of aniline being probably the rate determining step.[34] Observation of such a small ρ values indicates a weak substituent effect and a small contribution of arenium structure to the rate limiting step.[35] This is perfectly consistent with the calculations that suggest that the rate-determining barrier corresponds to the agostic C–H type transition structure (Figure 8).

Classical electrophilic aromatic substitutions that lead via a sigma complex (Wheland intermediate) with a highly developed positive charge at the aromatic ring have the ρ values around -10.[35] Pre-activated complex **4b** located on the pathway to the C–H activation can be interpreted as a Wheland-type intermediate. A gedanken experiment, in which formation of the pre-activated complex would represent the rate determining step, provides a Hammett plot with the ρ value of -2.7 (in red in Figure 5). The fact, that the experiments show ρ values in the range of -1.5 to -1.6 is clearly consistent with the rate determining step being the agostic C–H transition structure and not the Wheland type intermediate.

CONCLUSIONS

We present a new ESI-MS method for determination of rate constants of catalytic reactions in solution based on the investigation of a series of differently substituted substrates. The method is based on

mass-spectrometric detection of stable intermediates such as organopalladium complexes formed in C–H activation reactions. We have used the method for investigation of the cyclopalladation reaction of differently substituted acetanilides. The information on the reaction rates connected with the formation of the organopalladium complexes is extracted from time dependent mixing experiments of two reaction mixtures differing only in the substitution pattern of the reactants. The kinetic fitting of the results not only provides the required rate constants, but it also overcomes the problem of different ion transfer responses of differently substituted complexes during the electrospray ionization. Obtained rate constants were used for the construction of Hammett diagrams. We found a good correlation with the Hammett σ_m and σ_p^+ constants and the reaction constant ρ was determined as -1.5. The same reactions were investigated also by UV-VIS spectroscopy. We found the same trend in the Hammett diagram (ρ = -1.6), but the absolute rate constant were about three times smaller.

The theoretical calculations suggested that the C–H activation pathway leads via a pre-activated Wheland-type complex and that the rate determining barrier is represented by an agostic C–H transition structure. If the formation of a Wheland-type intermediate would be the rate limiting step, then the ρ value of -2.7 would be expected. The barrier represented by the agostic C–H transition structure gives a prediction of ρ = -1.7. The second scenario is clearly consistent with the experimental results.

ACKNOWLEDGEMENT

This work was supported by the Czech Science Foundation (14-20077S), European Research Council (ERC CoG No. 682275), and the COST action CHAOS. ZN acknowledges the support of the Hungarian Academy of Sciences (LP2012-48/2012)

Supporting Information

Influence of electrospray ionization and ion transfer efficiency, MS/MS spectra, visualized results of time-delay experiments, UV-Vis results and computational results together with geometries of all optimized structures.

REFERENCES

(1) Gensch, T.; Hopkinson, M. N.; Glorius, F.; Wencel-Delord, J. *Chem. Soc. Rev.* **2016**, *45*, 2900-2936 and references cited therein.

(2) (a) Roudesly, F.; Oble, J.; Poli G. *J. Mol. Catal. A: Chem.* **2017**, *426*, 275–296. And references cited therein (b) Roithová, J.; Schröder, D. *Chem. Rev.* **2010**, *110*, 1170 – 1211.

(3) (a) Chen, Z.; Wang, B.; Zhang, J.; Yu, W.; Liu, Z.; Zhang, Y. *Org. Chem. Front.* **2015**, *2*, 1107-1295. (b) Ryabov, A. D. *Chem. Rev.* **1990**, *90*, 403-424.

(4) (a) Lyons, T. W.; Sanford, M. S. *Chem. Rev.* **2010**, *110*, 114. (b) Ackermann, L. *Chem. Rev.* **2011**, *111*, 1315. (c) Liu, C.; Zhang, H.; Shi, W.; Lei, A. *Chem. Rev.* **2011**, *111*, 1780. (d) Kuhl, N.; Hopkinson, M. N.; Wencel-Delord, J.; Glorius, F. *Angew. Chem. Int. Ed.* **2012**, *51*, 10236. (e) Zheng, C.; You, S.-L. *RSC Adv.* **2014**, *4*, 6173. (f) Gensch, T.; Hopkinson, M. N.; Glorius, F.; Wencel-Delord, J. *Chem. Soc. Rev.* **2016**, *45*, 2900.

(5) (a) Lapointe, D.; Fagnou, K. *Chem. Lett.* **2010**, *39*, 1118-1126. (b) Gray, A.; Tsybizova, A.; Roithová, J. *Chem. Sci.* **2015**, *6*, 5544-5553. (c) Blackmond, D. G. *J. Am. Chem. Soc.* **2015**, *137*, 10852-10866.

(6) Ryabov, A. D.; Sakodinskaya, I. K.; Yatsimirsky, A. K. *J. Chem. Soc., Dalton Trans.* **1985**, 2629-2638.

(7) Davies, D. L.; Donald, S. M. A.; Macgregor, S. A. *J. Am. Chem. Soc.* **2005**, *127*, 13754-13755.

(8) (a) Gómez, M.; Granell, J.; Martinez, M. *Organometallics* **1997**, *16*, 2539-2546. (b) Gómez, M.; Granell, J.; Martinez, M. *J. Chem. Soc., Dalton Trans.* **1998**, 37-43.

(9) de Jong, G. T.; Geerke, D. P.; Diefenbach, A.; Bickelhaupt, F. M. *Chemical Physics* **2005**, *313*, 261-270.

(10) Flegeau, E. F.; Bruneau, C.; Dixneuf, P. H.; Jutand, A. *J. Am. Chem. Soc.* **2011**, *133*, 10161-10170.

(11) Boutadla, Y.; Davies, D. L.; Macgregor, A. A.; Poblador-Bahamonde, A. I. *Dalton Trans.* **2009**, 5820-5831.

(12) (a) Luinstra, G. A.; Wang, L.; Stahl, S. S.; Labinger, J. A.; Bercaw. J. E. *J. Organomet. Chem.*, **1995**, *504*, 75-91. (b) Agenet, N.; Amatore, Ch.; Gamez, S.; Gérardin, H.; Jutand, A.; Meyer, G.; Orthwein, C. *Arkivoc* **2002**, (v) 92-101.

(13) (a) Tunge, J. A.; Foresee, L. N. *Organometallics* **2005**, *24*, 6440-6444. (b) Jones, A. C.; Sanders, A. W.; Bevan, M. J.; Reich, H. J. *J. Am. Chem. Soc.* **2007**, *129*, 3492-3493. (c) Shekhar, S.; Ryberg, P.; Hartwig, J. F.; Mathew, J. S.; Blackmond, D. G.; Strieter, E. R.; Buchwald, S. L. *J. Am. Chem. Soc.* **2006**, *128*, 3584-3591. (d) Gonzalez, J. A.; Ogba, O. M.; Morehouse, G. F.; Rosson, N.; Houk, K. N.; Leach, A. G.; Cheong, P. H. Y.; Burke, M. D.; Lloyd-Jones, G. C. *Nat. Chem.* **2016**, *8*, 1067–1075.

(14) Theron, R.; Wu, Y.; Yunker, L. P. E.; Hesketh, A. V.; Pernik, I.; Weller, A. S.; McIndoe, J. S. *ACS Catal.* **2016**, *6*, 6911−6917.

(15) Ferretti, A. C.; Mathew, J. S.; Blackmond, D. G. *Ind. Eng. Chem. Res.* **2007**, *46*, 8584-8589.

(16) (a) Yunker, L. P. E.; Stoddard R. L.; Mclndoe J. S. *J. Mass Spectrom.* **2014**, *49*, 1–8. (b) Vikse, K. L.; Ahmadi, Z.; McIndoe J. S. *Coord. Chem. Rev.* **2014**, *279* 96–114.

(17) Janusson, E.; Hesketh, A.; Bamford, K.; Hatlelid, K.; Higgins, R.; McIndoe, J. S. *Int. J. Mass Spectrom.* **2015**, *388*, 1–8.

(18) Stokvis, E.; Rosing, H.; Beijnen, J. H. *Rapid Commun. Mass Spectrom.* **2005**, *19*, 401–407.

(19) Jašíková, L.; Anania, M.; Hybelbauerová, S.; Roithová, J. *J. Am. Chem. Soc.* **2015**, *137*, 13647-13657.

(20) Schulz, J.; Jašík, J.; Grey, A; Roithová, J. *Chem. Eur. J.* **2016**, *22*, 9827-9834.

(21) (a) Szabó, F.; Daru, J.; Simkó, D.; Nagy, T. Z.; Stirling, A.; Novák, Z. *Adv. Synth. Catal.* **2013**, *355*, 685-691. (b) Tremont, S. J.; Rahman, H. U. *J. Am. Chem. Soc*. **1984**, *106*, 5759-5760. (c) Wu, Y.; Li, B.; Mao, F.; Li, X.; Kwong, F. Y. *Org. Lett.* **2011**, *13*, 3258-3261. (d) Wu, Y.; Choy, P. Y.; Mao, F.; Kwong, F. Y. *Chem. Commun.* **2013**, *49*, 689-691. (e) Li, C.; Wang, L.; Li, P.; Zhou, W. *Chem. Eur. J.* **2011**, *17*, 10208-10212. (f) Jang, M. J.; Youn, S. W. *Bull. Korean Chem. Soc.* **2011**, *32*, 2865-2866. (g) Daugulis, O.; Zaitsev, V. G. *Angew. Chem. Int. Ed.* **2005**, *44*, 4046-4048. (h) Zhang, L.; Chen, K.; Chen, G.; Li, B.; Luo, S.; Guo, Q.; Wei, J.; Shi. Z. *Org. Lett.* **2013**, *15*, 10-13. (i) Szabó, F.; Simkó, D.; Novák, Z. *RSC Adv.* **2014**, *4*, 3883-3886. (j) Tischler, O.; Tóth, B. L.; Novák, Z. *Chem. Rec.* DOI: 10.1002/tcr.201600059. (k) Tischler, O.; Kovács, Sz.; Érsek, G. Králl, P.; Daru, J.; Stirling, A.; Novák, Z. *J. Mol. Catal. A: Chem.* **2017**, *426*, 444–450.

(22) Recrystalized palladium(II)acetate must be used.

(23) (a) Schulz, J.; Jašíková, L.; Škríba, A.; Roithová, J. *J. Am. Chem. Soc.* **2014**, *136*, 11513 – 11523. (b) Hývl, J.; Roithová, J. *Org. Lett.* **2014**, *16*, 200–203. (b) Schulz, J.; Jašík, J.; Gray, A.; Roithová, J. *Chem. Eur. J.* **2016**, *22*, 9827 –9834.

(24) Frisch, M. J.; Trucks, G. W.; Schlegel, H. B.; Scuseria, G. E.; Robb, M. A.; Cheeseman, J. R.; Scalmani, G.; Barone, V.; Mennucci, B.; Petersson, G. A.; Nakatsuji, H.; Caricato, M.; Li, X.; Hratchian, H. P.; Izmaylov, A. F.; Bloino, J.; Zheng, G.; Sonnenberg, J. L.; Hada, M.; Ehara, M.; Toyota, K.; Fukuda, R.; Hasegawa, J.; Ishida, M.; Nakajima, T.; Honda, Y.; Kitao, O.; Nakai, H.; Vreven, T.; Montgomery Jr., J. A.; Peralta, J. E.; Ogliaro, F.; Bearpark, M.; Heyd, J. J.; Brothers, E.; Kudin, K. N.; Staroverov, V. N.; Kobayashi, R.; Normand, J.; Raghavachari, K.; Rendell, A.; Burant, J. C.; Iyengar, S. S.; Tomasi, J.; Cossi, M.; Rega, N.; Millam, J. M.; Klene, M.; Knox, J. E.; Cross, J. B.; Bakken, V.; Adamo, C.; Jaramillo, J.; Gomperts, R.; Stratmann, R. E.; Yazyev, O.; Austin, A. J.; Cammi, R.; Pomelli, C.; Ochterski, J. W.; Martin, R. L.; Morokuma, K.;

Zakrzewski, V. G.; Voth, G. A.; Salvador, P.; Dannenberg, J. J.; Dapprich, S.; Daniels, A. D.; Farkas, Ö.; Foresman, J. B.; Ortiz, J. V; Cioslowski, J.; Fox, D. J. Gaussian 09, Revision D.01, Gaussian, Inc., Wallingford, CT, **2009**.

(25) Grimme, S.; Ehrlich, S.; Goerigk, L. *J. Comput. Chem.* **2011**, *32* (7), 1456–1465.

(26) Andrae, D.; Häussermann, U.; Dolg, M.; Stoll, H.; Preuss, H. *Theor. Chim. Acta* **1990**, *77* (2), 123–141.

(27) (a) Markert, Ch.; Pfaltz, A. *Angew. Chem. Int. Ed.* **2004**, *43*, 2498-2500. (b) Review: Müller, C. A.; Markert, Ch.; Teichert, A. M.; Pfaltz, A. *Chem. Commun.* **2009**, 1607-1618.

(28) Roithová, J.; Janková, Š.; Jašíková, L.; Váňa, J.; Hybelbauerová, S. *Angew. Chem. Int. Ed.* **2012**, *51*, 8378 –8382.

(29) (a) Mac Aleese, L.; Maître, P. *Mass Spectrom. Rev.* **2007**, *26*, 583–605. (b) Roithová, J. *Chem. Soc. Rev.* **2012**, *41*, 547–559.

(30) Luo, F.; Yang, J.; Li, Z.; Xiang, H.; Zhou, X. *Eur. J. Org. Chem.* **2015**, 2463–2469.

(31) Reed, C. A.; Kim, K.; Stoyanov, E. S.; Stasko, D.; Tham, F. S.; Mueller, L. J.; Boyd, P. D. W. *J. Am. Chem. Soc.* **2003**, *125*, 1796-1804.

(32) Konnick, M. M.; Gandhi, B. A.; Guzei, I. A.; Stahl, S. S. *Angew. Chem. Int. Ed.* **2006**, *45*, 2904 – 2907.

(33) (a) Barone, V.; Cossi, M. *J. Phys. Chem. A*, **1998**, *102*, 1995-2001. (b) Cossi, M.; Rega, N.; Scalmani, G.; Barone, V. *J. Comp. Chem.*, **2003**, *24*, 669-681.

(34) Chan, Ch.-W.; Zhou, Z.; Yu, W.-Y. *Adv. Synth. Catal.* **2011**, *353*, 2999-3006.

(35) Carey, F. A.; Sunberg, R. J. *Advanced Organic Chemistry Part A: Structure and Mechanisms*, fifth edition; Springer Science + Business Media; New York, **2007**, Chapter 9.